

# Navigation for the ACS3 solar sail mission

Andres Dono<sup>1\*</sup>, Ted Hendriks<sup>2</sup>, Keats Wilkie<sup>3</sup>

<sup>1</sup> Flight Dynamics Team Lead, *NASA Ames Research Center, Axient Corp., California, USA*

<sup>2</sup> Flight Dynamics Analyst, *NASA Ames Research Center, METIS LLC, California, USA*

<sup>3</sup> ACS3 Principal Investigator, *NASA Langley Research Center, Virginia, USA*

## Abstract

NASA's Advanced Composite Solar Sail System (ACS3) mission consists of a spacecraft that plans to be launched no earlier than April 2024. The spacecraft carries an 81 m<sup>2</sup> solar sail that can produce effective  $\Delta V$  to alter the initial 1000 km sun-synchronous orbit. The main objective of the mission is to demonstrate the capabilities of the solar sail to effectively change the semi-major axis of its initial orbit. Various composite materials were used to produce the sail, together with lightweight booms that will deploy from a 12U CubeSat bus.

The ACS3 navigation team at NASA Ames Research Center has built a Flight Dynamics System (FDS) to provide mission navigation and to produce regular ephemeris once in orbit. The FDS can compute the orbit transfers that the spacecraft will perform once the sail is deployed. To achieve that, GPS data is obtained from the spacecraft telemetry and then is used with a Kalman filter and a smoother to obtain an orbit determination solution. The outcome of this process reduces the position and velocity uncertainty in a daily cadence. After that, the state vector output is used to feed a propagation model that includes the updated attitude and orbit of the spacecraft at that given moment. The trajectory model considers the updated attitude plan of the spacecraft as well as the environment conditions such as the solar weather to compute the associated drag and solar radiation pressure. This paper explains in detail the implementation of the FDS, as well as the solar sail solar radiation pressure trajectory model. We also present the results of several potential trajectory models under various assumptions of orbit parameters, attitude, environment, and material properties. In addition, we introduce a trajectory model for potential interplanetary use of an equivalent solar sail in the future. The outcome of this process will be critical to achieving the objective of determining effective semi-major axis change produced by the solar sail.

## 1 INTRODUCTION

Solar sails constitute a relevant propulsive method for spacecraft, due to their capability of producing thrust without propellant. They utilize the exerted solar radiation pressure on their surface to generate a net force that, when oriented in a particular direction, can even result in large delta-V to enable interplanetary transfers. These trajectories would be in some cases not achievable with existing propulsion systems.

Solar sails have been implemented in several spacecraft missions for decades. Some of the first developments included the Znamya-2 solar sail deployment in space in 1993, the light solar sail structure ground demonstration that DLR and ESA performed in 1999, and the NASA/ATK L'Garde ground sail demonstration in 2004. The IKAROS mission in 2010 was a major development. This mission was relevant since it demonstrated the effectiveness of a solar sail propulsive method to do a large interplanetary transfer by completing a Venus flyby in 2010. NanoSail-D was launched also in 2010. This mission, developed jointly at NASA's Ames and Marshall centers, consisted of a solar sail of 10 m<sup>2</sup> stocked in a 3U CubeSat. This spacecraft demonstrated the capabilities of such a sail as a drag device [1]. The LightSail missions were launched in 2015 and 2019 respectively. These missions, developed by the Planetary Society, were a successful demonstration of a solar sail in LEO. LightSail-1 was a technology demonstration mission that tested the sail deployment in LEO. The follow-up mission, LightSail-2 was able to perform effective semi-major axis increase by a measurable amount. It was placed in a 720 km altitude orbit and the spacecraft performed attitude control to orient the sail relative to the Sun. Each LightSail spacecraft had a 32m<sup>2</sup> solar sail made of mylar [2].

Other relevant sail developments included the Sunjammer mission, which consisted of a solar sail of as much as 1200 m<sup>2</sup> to be operated as maintenance propulsive method in a Lagrange point. The sail was developed by L'Garde and NASA, and it was also intended to capture coronal solar mass ejections. The project was concluded in 2014, with relevant lessons learned and project development data that were captured for further NASA missions [3]. The Solar Cruiser mission, developed at NASA Marshall and Ball Aerospace, proposed to carry an even larger solar sail of 1653 m<sup>2</sup>. The project achieved a successful deployment of a solar sail quadrant [4]. The NEA Scout spacecraft carried a solar sail developed also at NASA Marshall and launched aboard the maiden flight of SLS, as part of the Artemis-1 secondary spacecraft campaign. NEA Scout had the mission objective to perform a lunar flyby and gain enough energy to arrive to an asteroid. The sail would be used as a steering propulsive method to obtain the required delta-V to perform a flyby of the asteroid 2020 GE [5]. However, the ground segment did not receive telemetry upon deployment from the upper stage launch vehicle, therefore the sail performance could not be measured. Current investigations are ongoing to find out the cause of the spacecraft loss of communication.

The ACS3 mission builds upon this long heritage of developments in space sailing. It consists of a 12U CubeSat form factor spacecraft developed by the company Nanoavionics, located in Lithuania. The spacecraft is going to be launched aboard an Electron launch vehicle from Mahia, New Zealand, no earlier than April 2024. This paper includes an overview of the spacecraft design and concept of operations (ConOps). The navigation of the spacecraft will be provided by the flight dynamics team, located at NASA Ames. Therefore, this paper will place a special emphasis on the development and initial tests of the flight dynamics system (FDS) that was custom built for the mission. The later sections will outline the orbit determination process during nominal operations, and the propagation of the spacecraft trajectory once the solar sail is deployed.

## 2 ACS3 SPACECRAFT

ACS3 plans to be the first on-orbit test of the new generation of NASA’s composite booms, that have a compact design to fit in small spacecraft buses where including deployable structures is challenging. The main objective of the mission, developed and led by NASA Langley and Ames Research Centers, is to perform a successful deployment of the composite boom solar sail in LEO. An on-board camera system will enable the analysis of the images during and after the deployment phase. Once that is completed, extended goals include to demonstrate the sail performance as a method of propulsion by achieving controlled orbit raising and lowering. The solar sail has a 81 m<sup>2</sup> surface area and is formed by four quadrants, made of metallized polyethylene naphthalate (PEN) thin films that are just 2.115 micro meters thick [6].

The ACS3 spacecraft has a 12U CubeSat form factor size. The spacecraft bus contains the flight computer, the ADCS, communications and power subsystems. For ADCS, the spacecraft uses four reaction wheels, three 3-axis magnetorquers, six sun sensors, a GPS receiver, a star tracker and an inertial measurement unit. Communications are performed with a UHF radio, four UHF antennas and a S-band transceiver. In addition, a payload electronics board and four cameras are carried in each spacecraft surface face are used for sail diagnostics. The main payload consists of the Sail-Boom Subsystem (SBS), that includes the stowed composite booms and solar sail quadrants. Figure 1 shows an outline of the spacecraft bus and SPS subsystem, while Figure 2 shows the actual sail fully deployed on a ground demonstration test [6].

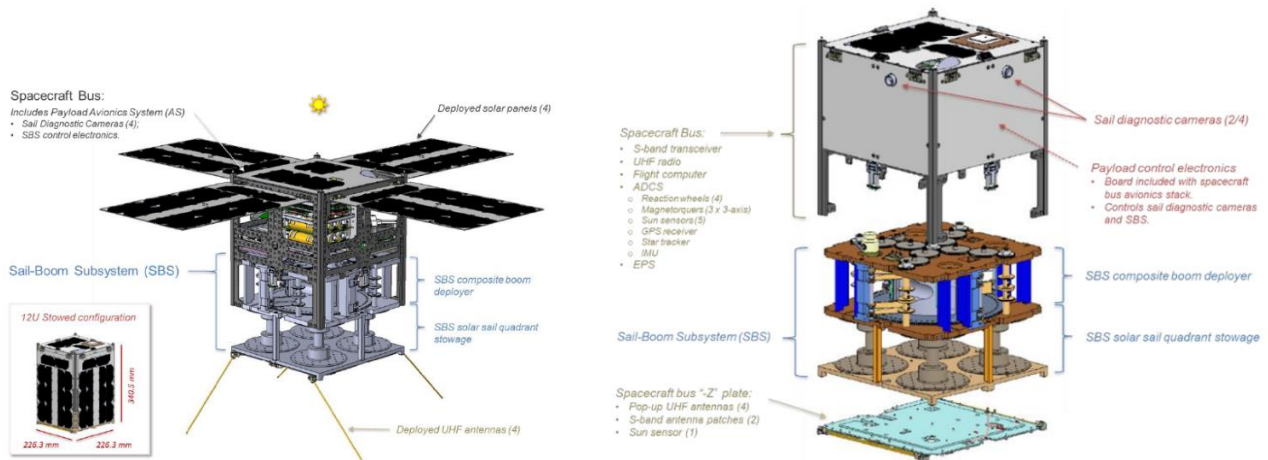


Figure 1: On the top, the spacecraft sail bus subsystem configuration showing the location of the composite booms and the solar sail stowage. On the bottom, a breakdown of the various spacecraft bus subsystems [6].



Figure 2: Solar Sail fully deployed at the test facility at NASA Langley Research Center [6].

### 3 MISSION CONCEPT OF OPERATIONS

The spacecraft will be inserted in a circular sun-synchronous orbit, at 1000 km altitude and 97.8 degrees of inclination. The Local Time of Descending Node (LTDN) window will be 10:30-11:30 AM. This time was carefully selected to increase the amount of sunlight during the solar sail phase of the mission, since the sail will need to be pointing at the Sun to generate thrust. In particular, the delta-V imparted by the solar radiation pressure, will need to have a component in the velocity direction to raise the orbit of the spacecraft.

The ConOps includes the spacecraft separation from the launch vehicle hours after launch, which is established at a tentative date no earlier than the 24<sup>th</sup> of April 2024. The launch vehicle is an Electron from the company Rocket Lab. The launch site is in Mahia, New Zealand. At the time of the publication of this paper, the spacecraft was shipped to the launch facility, and it is being integrated into the payload fairing. The separation will be imparted by a spring mechanism with sufficient delta-V to avoid recontact. Once the spacecraft is deployed, the launch and early operations phase (LEOP) starts from L-0 to L+60 days, and the spacecraft will be operated from the ground facility to perform its detumble sequence and to check to make sure all the subsystems are functioning correctly. ACS3 will be then in its initial orbit for a period of two months until the next critical phase.

At L+61 days, the sail deployment will be commanded from the ground station. The process is automated once it is activated, and it is expected to last approximately 30 minutes. The deployment will take place during optimal sun angle conditions, and the spacecraft attitude will be sun-pointing. During five days, spacecraft operators will check that it has been completed successfully.

During the follow up phase, from L+66 to 90 days, a structural dynamics characterization experiment of the deployed sail will be performed. Imagery of the sail deployment will be prioritized for the

downlink passes. During this period, the team will attempt calibration maneuvers to study the various forces affecting the sail propagation. Table 1 includes a list of the candidate calibration maneuvers:

<b>Sail maneuver name</b>	<b>Description</b>	<b>Purpose</b>
<b>Constant 0 deg</b>	Maintaining sail attitude at 0 deg cone angle	Calibration of the maximum sail acceleration
<b>Constant 35.3 deg</b>	Maintaining sail attitude at 35.3 deg cone angle	Characterization of the transverse sail acceleration
<b>180 deg turn</b>	Continuous attitude changes across cone angle domain: (-90,90) deg	Study of the transverse and radial acceleration profiles with respect to the Sun-sail vector
<b>Albedo</b>	Nadir pointing during direct sunlight	Study the effects of Earth albedo
<b>BBR</b>	Nadir pointing during eclipse conditions	Study of the effects caused by black-body radiation
<b>Max Drag</b>	Fixed sail attitude at normal vector opposite to velocity vector	Calibration of the maximum acceleration due to atmospheric drag at the nominal orbit
<b>90 deg turn</b>	Changing attitude during eclipse, across the angle of attack domain: (0,90) deg	Study of the profile of transverse and radial drag accelerations with respect to the velocity vector
<b>Zero force</b>	Sail normal vector along the angular momentum vector	Study of other residual forces

Table 1: Candidate calibration maneuver description.

Once the sail has been fully deployed and calibrated, the orbit-raising mode will be started, from L+91 to L+110 days. For approximately a month, the spacecraft will attempt to raise its semi-major axis to demonstrate the sail performance to alter this orbital element. The opposite maneuver will be performed as well right after, from L+111 to L+130 days, to decrease the semi-major axis in a controlled manner. Once those two main propulsive events are completed, the spacecraft will be entering its decommissioning phase, occurring from L+131 to L+181 days. The goal of this last phase will be to decrease the semi-major axis to initiate re-entry. This end-of-mission phase will be coordinated in conjunction with the NASA Conjunction Assessment Risk Analysis (CARA) office. This process involves on-going spacecraft ephemeris propagation analysis to ensure that the ACS3 spacecraft is ready for passivation. Therefore, the flight dynamics team will have to calculate the descent plan and trajectory for an active controlled approach, where the spacecraft can be steered to obtain a controllable delta-V from drag and SRP, and for also a passive approach, where the spacecraft is assumed to be turned off, and therefore subject to tumbling. Prior to the completion of the descent plan, ACS3 team will have to mitigate any potential risk associated with orbital crossings with the ISS or other orbiting spacecraft. Passivation of the ACS3 spacecraft is commanded by making the solar panels to stop charging the batteries, draining the batteries consequently.

The end-of-mission phase will span from L+182 to L+192 days. At this stage, no contact will be established with the spacecraft. Therefore, maneuvering capabilities will not be available. The drag force will be significant and depending on various factors such as the spacecraft ballistic coefficient and the solar weather will determine the final re-entry time. Figure 3 includes a lifetime prediction of

the potential time that may take the ACS3 spacecraft to achieve re-entry, under the uncontrolled deorbiting assumption. The active approach is also shown for comparison purposes.

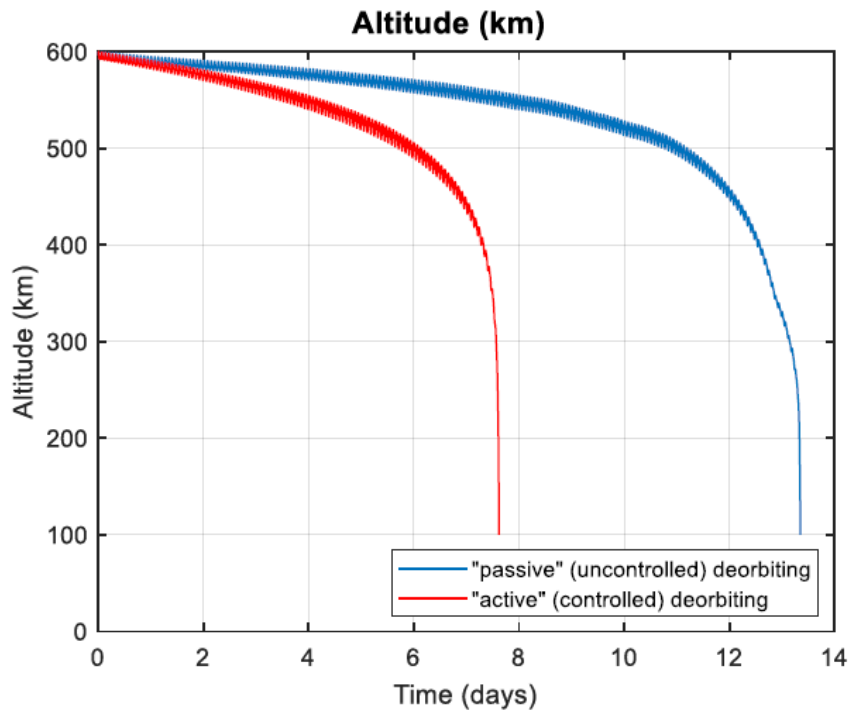


Figure 3: Reentry time from 600 km altitude. The red curve corresponds to an active approach where the drag force and the SRP are used to accelerate the reentry. The blue curve corresponds mostly to the drag force acting in the sail and spacecraft.

## 2 FLIGHT DYNAMICS SYSTEM

The ACS3 flight dynamics team is responsible for the navigation of the spacecraft. To achieve that, the team gathers the recurring tracking data provided by the spacecraft telemetry, performs orbit determination, and then generates the predicted satellite ephemeris. The team utilizes an automated Flight Dynamics System (FDS) tool, built in-house, to execute these steps.

The tool is written in Python and provides an automated structure for all the navigation tasks. It consists of three major components, the file processor, the orbit determination manager, and the propagation manager. The file processor handles all data synchronization between the different components of the FDS and the external data stakeholders. The orbit determination manager ensures that the satellite force model, smoother, and filter are all configured properly. Additionally, it performs orbit determination and provides quality control reports and graphs. The propagation manager receives the orbit determination solution and generates historical orbit plots, attitude predictions, predicted orbit plots, and conjunction screening products.

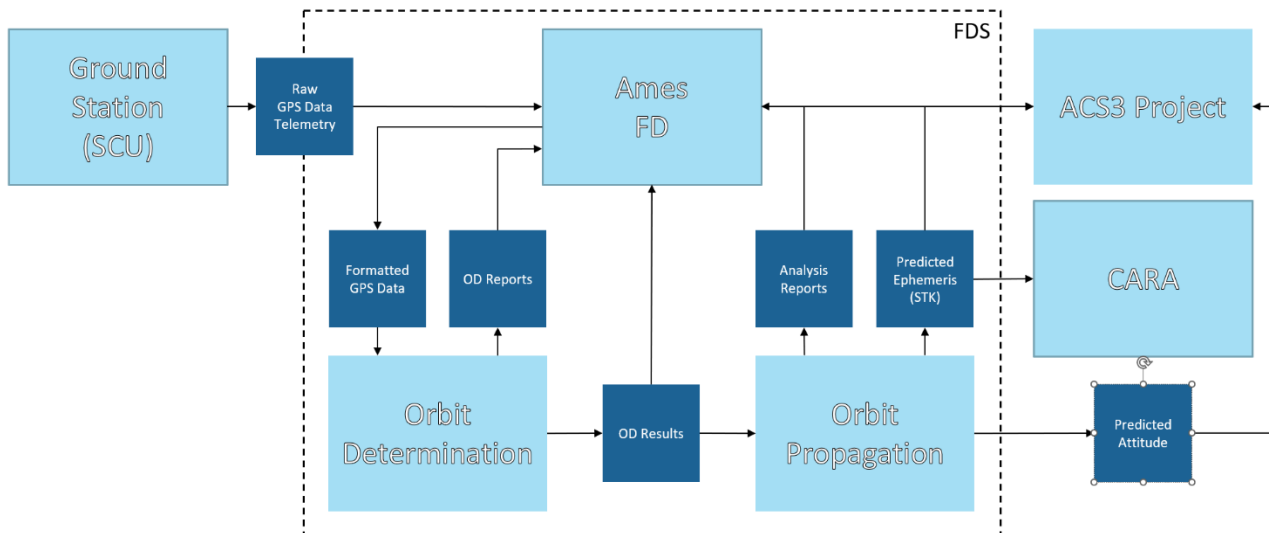


Figure 4: Flight Dynamics System Overview.

Figure 4 outlines how the data architecture is transferred within the FDS. Measurements are delivered to the NASA Ames FD team after each ground pass and processed by the tool. The ground station facility is located at Santa Clara University (SCU), in California. Each day there are two passes to gather spacecraft telemetry and upload commands. Orbit determination is automatically performed, with quality control products reported to the FD team and the processed satellite orbit ephemeris is made available. The propagation manager sets its initial state vector from this ephemeris and generates an updated predictive solution based on the expected spacecraft orientation. Orbit analysis reports that include all the orbital elements evolution are produced for the larger ACS3 mission team. A predicted orbit ephemeris with a  $6 \times 6$  covariance matrix of position and velocity uncertainty is provided to NASA CARA daily for conjunction screening. The FDS also provides automatically a TLE based on the GPS ephemeris solution, that is later utilized by the ground station facility to obtain a more accurate prediction of the access times to the spacecraft in the following passes.

### 3 ORBIT DETERMINATION

Once the spacecraft separates from the launch vehicle, an initial state vector is provided by the launch vehicle to be used for Initial Orbit Determination (IOD). Using the batch least squares technique, the flight dynamics team will generate an initial ephemeris during this first phase. Once that occurs, the software will feed the generated solution to a Sequential Kalman Filter that is going to be utilized during the rest of the mission.

Nominally, the spacecraft will record GPS measurements and attitude quaternions once per minute. These data are downlinked at the SCU ground station twice per day and passed to the flight dynamics team when it becomes available at the ground station. The GPS measurements and attitude quaternions from the spacecraft telemetry are processed into formats used by the FDS. In the orbit determination process, the measurements are used to feed the Kalman filter first. The filter output is then processed by a Rauch-Tung-Stribel sequential smoother. This results in a more accurate ephemeris that populates the initial state of the satellite propagation process.

## Output Products and Quality Control

To plan spacecraft operations, evaluate solar sail performance, and generate orbit predictions, the FDS generates reports and graphs at various stages. During the orbit determination process, measurement residuals, residual ratios, position uncertainty, and velocity uncertainty plots provide insight into the solution convergence and confidence in the produced ephemeris. This section includes an example of these plots from one of the operational readiness tests (ORTs) to prepare for the mission prior to launch, and performed with simulated GPS tracking data.

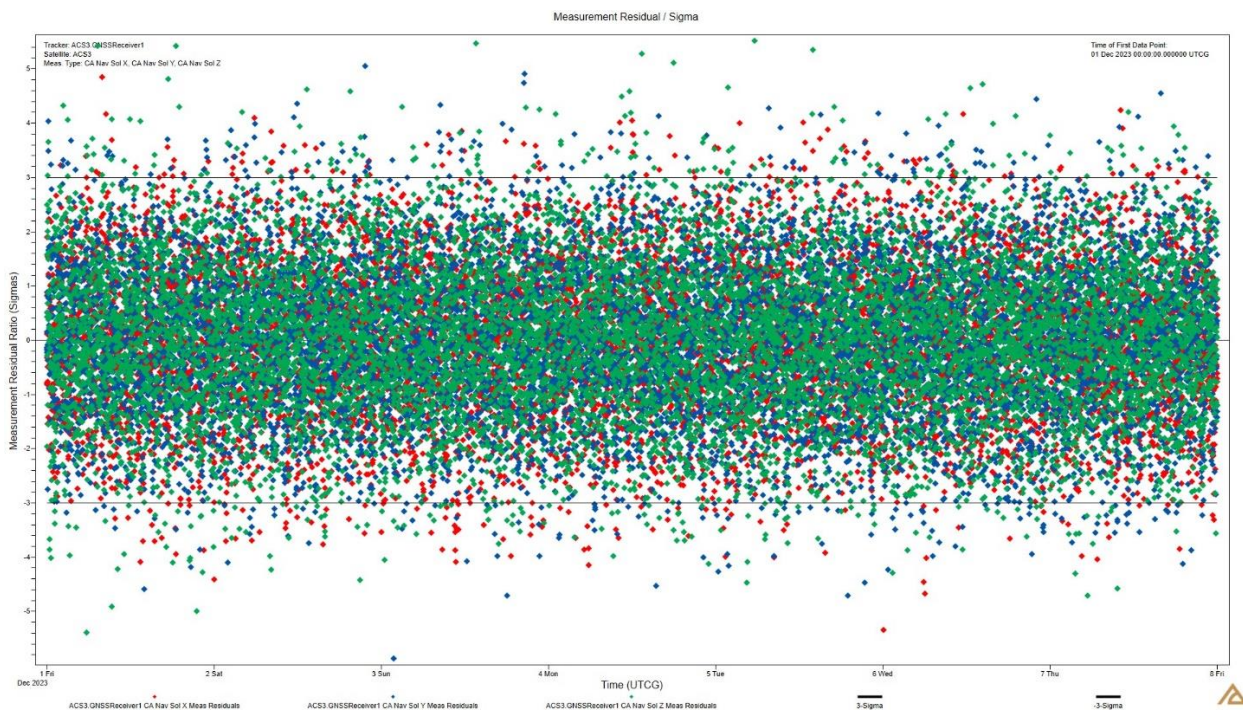


Figure 5: Example output measurement residual plot from ODTK. This image includes simulated tracking data from one of the ORTs performed prior to launch, as preparation for the mission and for testing purposes of the FDS.

As seen in Figure 5, measurements residual ratios plots allow the flight dynamics team to gauge the accuracy of the orbit determination solution. This figure was generated with simulated tracking data that spans 1<sup>st</sup> Dec 2023 to 8<sup>th</sup> Dec 2023 at a sixty seconds time step. Simulated tracking data utilized for this test included uncertainties such as measurement white noise and bias errors.

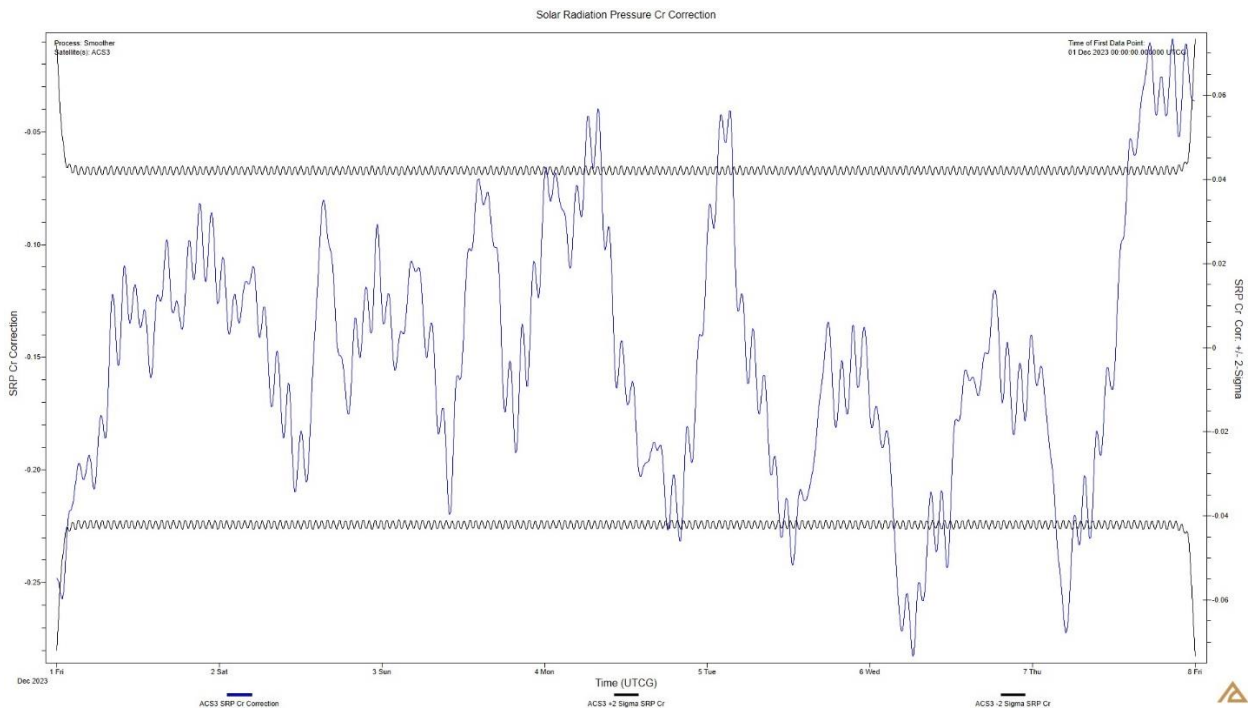


Figure 6: Solar Radiation Pressure correction plot from ODTK. This plot represents the smoother solution for one of the ORTs, performed with simulated GPS tracking data.

As seen in Figure 6, the orbit determination process computes the solar radiation pressure correction as a result of the smoother solution. This plot is used to evaluate the solar sail model used in the flight dynamics team. A similar report is produced for the ballistic coefficient, which will become more relevant in the later stages of the mission, once the spacecraft will be at lower altitudes and hence be exposed to a more substantial drag force.

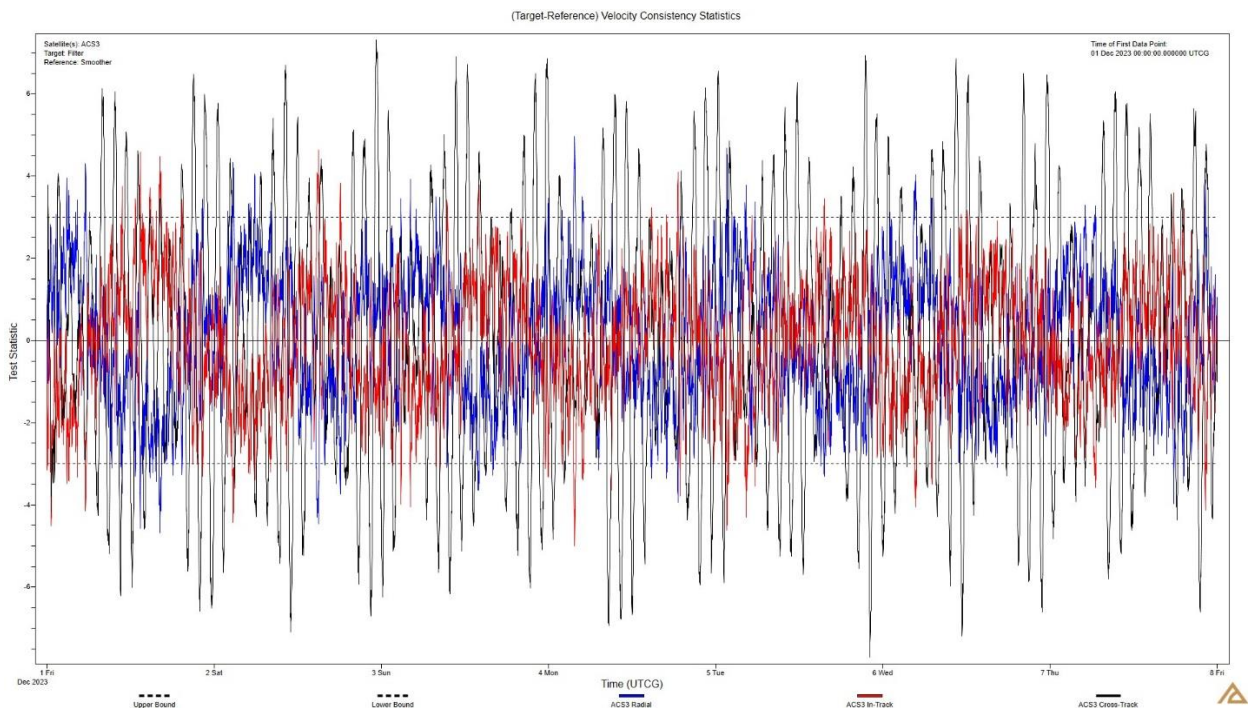


Figure 7: Example velocity consistency plot from ODTK.

As seen in Figure 7, the consistency plots demonstrate the agreement between the filter and smoother solutions, while Figure 8 corresponds to the position and velocity uncertainties of the filter and smoother process. The FDS provides consistency plots for position, velocity, solar radiation pressure corrections, and ballistic coefficient corrections.

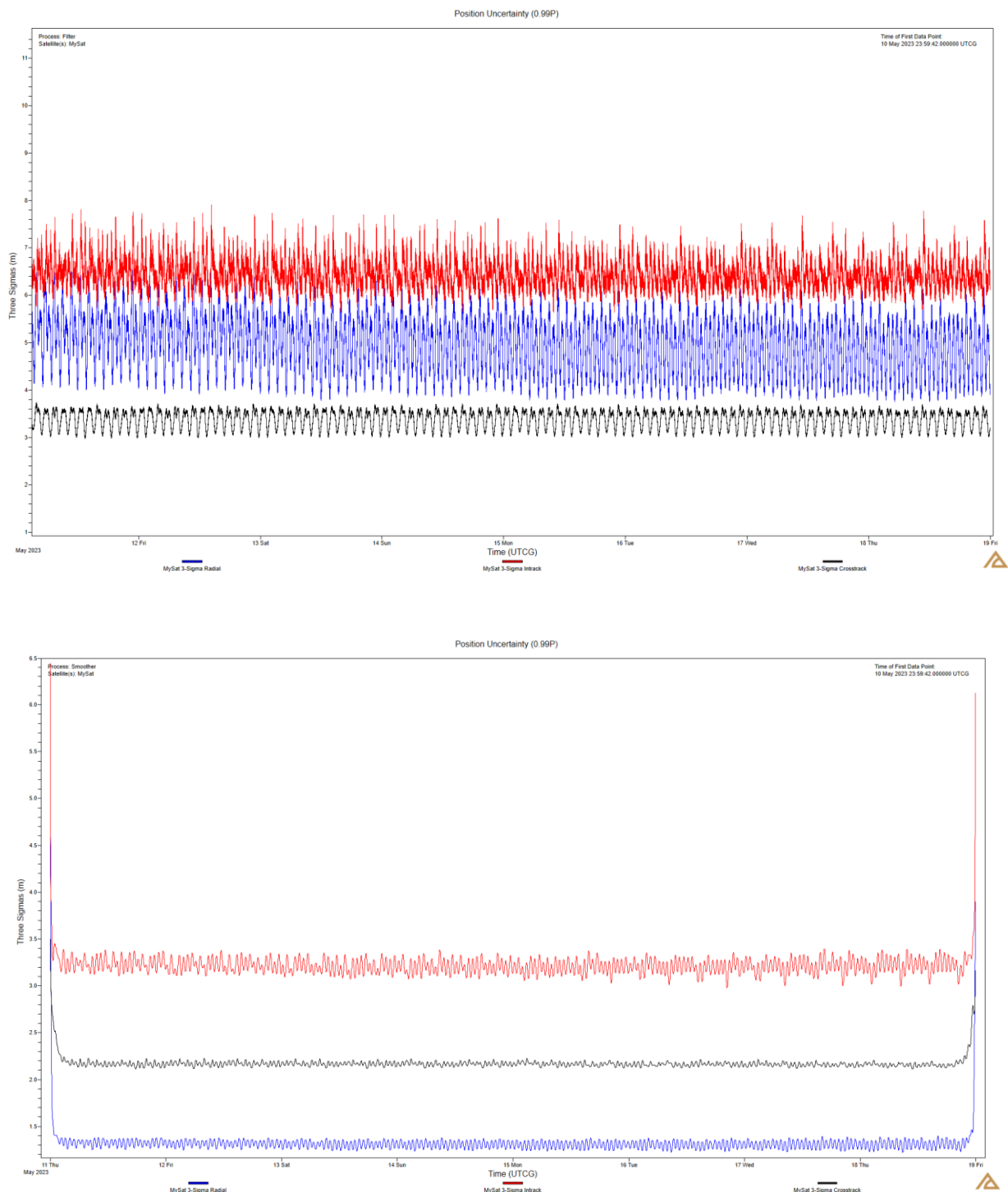


Figure 8: On the top, the position uncertainty obtained after the filter orbit determination process after a day's worth of tracking data from the GPS. On the bottom, the smoother is able to improve the results. These plots correspond to a test done with simulated tracking data. The measurement cadence was 60 seconds.

## 4 ORBIT PROPAGATION

Once the orbit determination is performed, a new ephemeris based on actual tracking data is obtained. This new solution can be utilized to generate a predictive ephemeris, based on a solar sail propagation model. The FDS propagator consists of a EMG2008 gravity model with 21x21 harmonics, a NRLMSISE00 atmospheric model, an SRP plate model, and with third body gravity effects from the Moon and the Sun. The propagator includes daily updated data such as solar weather coefficients and estimates of the ballistic coefficient based on the solution obtained by the orbit determination. Therefore, the initial state and updated coefficients are used to start the orbit propagation for a total of seven days, for NASA CARA screening purposes and to generate meaningful data for the mission and ground system. A new ephemeris with also covariance uncertainty propagation is then generated and provided to the mission in SPICE format and to CARA in CCSD v2.0 format. In addition, Two-Line Elements (TLE) are also generated for the ground station facility at SCU. This process occurs daily and each ephemeris is accompanied by a complete report with results regarding the change in orbital elements, ground pass schedules and any other relevant data for the mission such as eclipse times for power budget planning.

There are two main phases for orbit propagation during the mission. The first one corresponds to the mission phases prior to sail deployment, during commissioning when the sail is stowed. At this stage, the spacecraft is modelled as a 12U CubeSat with fold out solar panels, and therefore the effects of SRP are not as prominent, and the propagation can be done in a more simple manner.

The second phase starts when the sail is deployed. Therefore, the FDS includes the sail SRP propagation in the orbit prediction. After sail deployment, the spacecraft attitude has a large impact on the predicted trajectory. The FDS then computes optimal sail sun-pointing times and quaternions, and reports those to the mission operators for spacecraft attitude command generation.

The FDS will plan to use two techniques. The first one uses a simple approach where the spacecraft locks an attitude for an extended time during the orbit and then switches it when the sun conditions enable the sail to generate thrust. In this scenario, to raise the orbit, the sail normal vector has to be aligned with the Sun vector when a component of the sun position vector is aligned with the satellite's positive velocity vector and the sail is not in shadow. These conditions are met when the spacecraft is crossing the x-y plane of the ecliptic plane until it enters an eclipse period caused by the Earth's umbra. Figure 8 includes the result of a simulation that utilizes this technique. This plot presents the mean semi-major axis of a 90-day simulation. For the first 60 days, the vehicle has no sail, for the last 30 days the is modelled with a sail. Attitude profiles were computed by the FDS for the orbit raising portion of the mission.

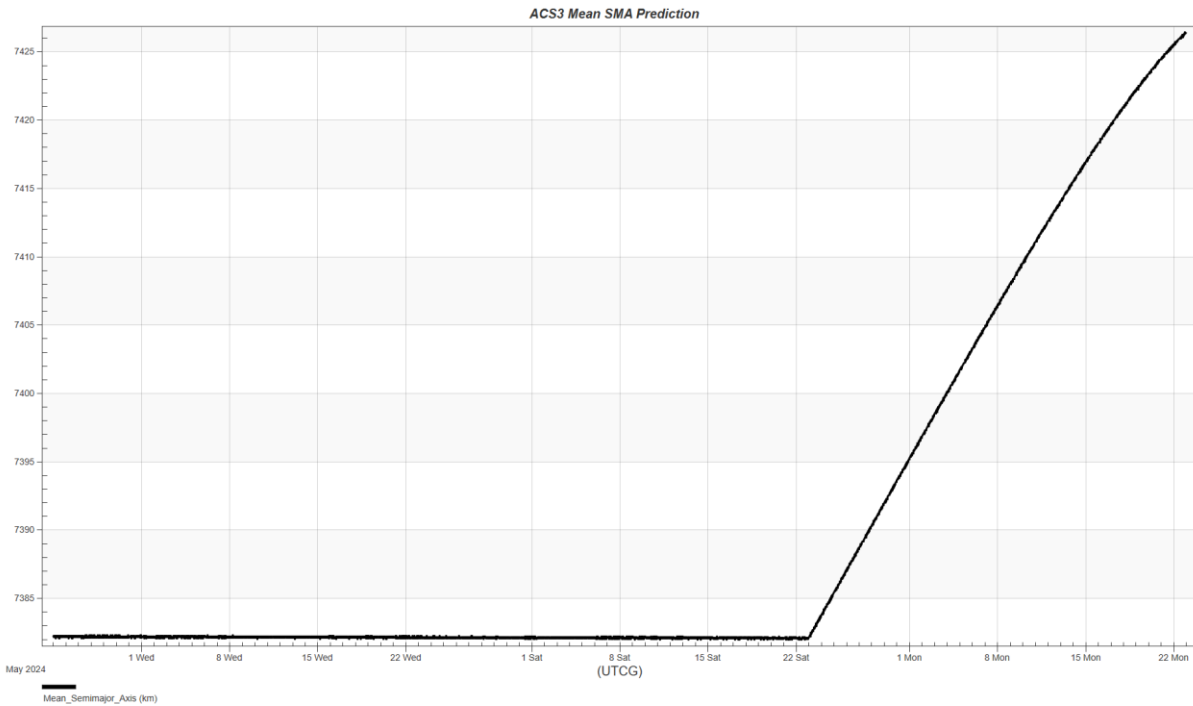


Figure 8: 90-day simulation of satellite. 60 days commissioning and satellite check out, 30 days of orbit raising.

Alternatively, for orbit lowering, the satellite follows a similar pointing scheme except the sail normal vector must be parallel to the sun vector when a component of the sun position vector is aligned with the satellite’s negative velocity vector. These conditions are satisfied when the spacecraft has exited an eclipse period until it crosses the x-y plane of the ecliptic. In both cases, the satellite will have to update its attitude profile twice an orbit. The FDS will compute the ecliptic crossing times, umbra entrance times, and umbra exit times and generate an attitude profile update plan.

To model the SRP forces, the FDS uses a plate model that consist of a superposition of various planes with distinct physical properties. These planes define the various faces of the spacecraft, the solar panels, and the sail, since they have different surface areas and materials. For instance, the front and back of the solar sail are defined by different reflectance coefficients.

The other technique that the FDS plans to use corresponds to the optimal locally steering law introduced by McInnes [8]. This law is defined by Equation 1, and it has the capability to locally calculate the optimal pitch angle for steering at a given time, based on the angle of the velocity vector with respect to the sun line.

Locally optimal sail pitch angle.      Angle of velocity vector with respect to sun line.

$$\alpha^* = \frac{1}{2} \left[ \psi - \sin^{-1} \left( \frac{\sin \psi}{3} \right) \right]$$

Equation 1: McInnes locally optimal steering law.

## 5 CONCLUSION

The ACS3 spacecraft is set to launch in April 2024. It will be inserted in a 1000 km circular sun-synchronous orbit. It carries an 81 m<sup>2</sup> solar sail that will be utilized as a main propulsive method to raise and then lower its semi-major axis. That performance will be measured by analyzing the tracking data provided by the onboard GPS hardware. The flight dynamics team at NASA Ames has built a custom FDS to ensure the robustness of that process and to automate the daily navigation operations. The system will acquire the daily measurements, produce orbit determination, and generate an ephemeris with covariance for collision avoidance purposes. In addition, the system will analyze the status of the spacecraft orbital elements, as well as produce an update on the subsequent ground station passes. Once the sail is deployed, the system will also compute the required propagation and attitude changes to ensure mission success in the form of suitably changed the spacecraft attitude at specific times to produce effective delta-V for orbit raising and lowering.

This paper includes details about the FDS implementation and process at the various stages during the mission. Plots with simulation tracking data from the mission rehearsal operational readiness tests have been shown, prior to launch. Future work will include already processed data from the mission telemetry.

## 6 ACKNOWLEDGEMENTS

The authors of this paper would like to thank the Space Flight Division and the ACS3 team at NASA Ames Research Center for supporting this publication. We would like to highlight the support from Alan Rhodes and Rudy Aquilina during all the preparation prior to launch. We would like to thank as well the ADCS team at NASA Marshall Space Flight Center for regular and useful discussions regarding the implementation of our FDS, in particular Andrew Heaton and Ben Diedrich. Lastly, thanks to the ground segment team at SCU for providing useful information for our simulations.

## 7 REFERENCES

- [1] Johnson, Les. ‘Solar Sail Propulsion For Interplanetary Small Spacecraft’. SP2018-00017, NASA Marshall Space Flight Center.
- [2] Spencer D. et al. ‘The LightSail 2 Solar Sailing Mission Summary’. 37th Annual Small Satellite Conference. SSC23-WVIII-01. Logan, Utah, 2023.
- [3] Barnes, Nathan & Derbes, William & Player, Charles & Gohardani, Amir. (2014). Sunjammer: A State-of-the-Art Space Mission. AIAA SPACE 2014 Conference and Exposition. 10.2514/6.2014-4170.
- [4] James B. Pezent, Rohan Sood, Andrew Heaton, Kyle Miller, Les Johnson, Preliminary trajectory design for NASA’s Solar Cruiser: A technology demonstration mission, *Acta Astronautica*, Volume 183, 2021, Pages 134-140, ISSN 0094-5765.
- [5] T. R. Lockett *et al.*, "Near-Earth Asteroid Scout Flight Mission," in *IEEE Aerospace and Electronic Systems Magazine*, vol. 35, no. 3, pp. 20-29, 1 March 2020, doi: 10.1109/MAES.2019.2958729.
- [6] Wilkie, Keats. ‘The NASA Advanced Composite Solar Sail System (ACS3) Flight Demonstration: A Technology Pathfinder for Practical Smallsat Solar Sailing’. 35th Annual Small Satellite Conference. SSC21-II-10.
- [7] Turyshche et al. ‘Science opportunities with solar sailing smallsats’.
- [8] McInnes, C. R., "Solar Sailing: Technology, Dynamics and Mission Applications," Springer- Praxis Books in Astronautical Engineering, Springer-Verlag, Berlin, 1999.